Experimental demonstration of optical real-time data compression[a)]

Mohammad H. Asghari[1,b)] and Bahram Jalali[1,2,3]
[1]*Department of Electrical Engineering, University of California, Los Angeles, 420 Westwood Plaza, Los Angeles, California 90095, USA*
[2]*Department of Bioengineering, University of California, Los Angeles, 420 Westwood Plaza, Los Angeles, California 90095, USA*
[3]*Department of Surgery, David Geffen School of Medicine, University of California, Los Angeles, 420 Westwood Plaza, Los Angeles, California 90095, USA*

(Received 7 January 2014; accepted 3 March 2014; published online 17 March 2014)

We experimentally demonstrate a method for compressing the time-bandwidth product of analog signals in real-time. By performing self-adaptive stretch, this technology enables digitizers to capture waveforms beyond their bandwidth with digital data size being reduced at the same time. The compression is lossless and is achieved through a transformation of the signal's complex field, performed in the analog domain prior to digitization. For proof of concept experiments, we compress the modulation bandwidth of an optical signal by 500 times. At the same time, we reduce its modulation time-bandwidth product (i.e., the record length) by 2.73 times while achieving 16 dB power efficiency improvement in comparison to the case of using conventional dispersive Fourier transform. Dispersive data compression addresses the big data problem in real-time instruments and in optical communications. © *2014 AIP Publishing LLC*.
[http://dx.doi.org/10.1063/1.4868539]

In conventional digitizers, the analog signal is sampled at twice the highest frequency of the signal, the so-called Nyquist rate. This results in two problems: (1) it limits the maximum frequency that can be captured to half the sampling rate and (2) unnecessarily long digital record length because frequency components below the Nyquist rate are oversampled creating a "big data" problem in real-time instruments. The relevant figure of merit is the product of the record length and the bandwidth, known as the Time-Bandwidth Product (TBP). This central figure of merit determines the number of samples, and hence the digital data size, required to represent the original information. This is the quantity we aim to modify.

Time Stretch Dispersive Fourier Transform (TS-DFT) offers a solution for the first problem of Nyquist sampling by slowing down the signal in time so it can be captured with a digitizer that otherwise would be too slow.[1] It is based on using a dispersive element to reduce the signal envelope bandwidth.[1] TS-DFT in the far-field regime emulates Fourier transformation[1–3] so it can be used as a real-time spectrometer. TS-DFT has been shown to be a powerful method for real-time high-throughput spectroscopy,[4,5] imaging and microscopy,[6–8] and wideband A/D conversion.[9–12] Owing to high-throughput operation, these instruments generate massive amounts of data (as high as 1 Tbit/s) creating a severe big data problem in detection, storage, and processing. Time Stretch Transform (TST) or Coherent Dispersive Fourier Transform (CDFT) combines TS-DFT with coherent detection and is able to measure both time domain and spectral profile of signals with high-throughput.[13–18] TST operates in both near-field[13] and far-field[14–18] regimes. To date, in all high throughput instruments, the TBP remains constant so the big data problem associated with Nyquist sampling remains unsolved.

In this letter, we experimentally demonstrate our recently proposed transformation that solves both problems of Nyquist sampling by compressing the time-bandwidth product. The proposed transform warps the signal's complex field in the analog domain before sampling and digitization.[19–21] The so-called Anamorphic Stretch Transform (AST) performs self-adaptive stretch by reshaping the signal with a nonlinear transformation. The signal reshaping is then combined with complex field detection followed by digital reconstruction. The net result is that the modulation bandwidth is reduced without the aforementioned expense of a proportional increase in temporal duration. One of the steps in AST is nonlinear frequency-to-time mapping in both near-field and far-field regimes, so it can be referred to as warped near-field transform and warped dispersive Fourier transform, respectively. However, this by itself does not cause a change in time-bandwidth product and cannot perform data compression. AST combines nonlinear frequency-to-time mapping with a nonlinear operation in the photo diode, i.e., envelope detection, to compress the TBP.

Fig. 1 compares our proposed method with mentioned techniques for reducing the envelope bandwidth of optical signals. We note that the anamorphic stretch has optical signal as its input. In contrast, the photonic time stretch analog to digital converter[12] has an electrical input. A method for the use of AST in the photonic time stretch digitizer was proposed in Ref. 21. In the experimental results shown in this letter, we use AST to compress the modulation bandwidth of an optical signal by 500 times. At the same time, we reduce its TBP (i.e., the record length) by 2.73 times while achieving 16 dB power efficiency improvement in comparison to the case of using time stretch transform.

For proof-of-the-concept experiments, we aim to compress the modulation bandwidth of an input analog signal

[a)]An earlier and brief version of this work was presented in the post-deadline session at Frontiers in Optics Conference in Orlando, December 2013 [22].
[b)]Email: asghari@ucla.edu.

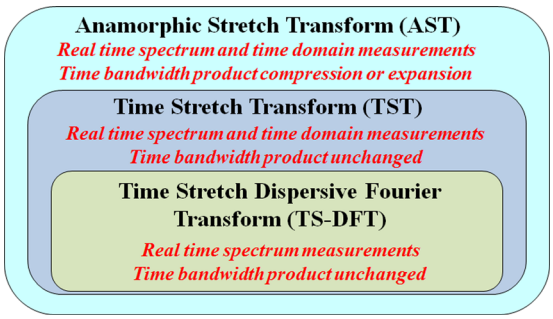

FIG. 1. TS-DFT and TST are special cases of the AST. TS-DFT provides information about the signal spectrum in real time. TST provides information about the signal in the time domain and spectral domain in real time. AST provides information about the signal in the time domain and spectral domain in real time with reduced record length, i.e., time bandwidth product compression. AST can be also used to expand the time bandwidth product.

while minimizing its duration. The experimental setup is shown in Fig. 2. The experiments compare the TBP of the signal for the case of using filter with nonlinear group delay (GD), i.e., AST, and with linear GD, i.e., TST. The particular shape of the AST filter GD profile is designed from a 2D distribution plot called modulation intensity distribution or stretched modulation (S_M) distribution (see Fig. 2 in Ref. 19). S_M plots suggest that for time-bandwidth compression, the AST filter GD profile should be a sublinear function of frequency. The $\tan^{-1}$ function provides a simple mathematical description of such GDs (for more information, refer to Ref. 19). The nonlinear GD is experimentally realized using a custom chirped fiber Bragg grating (CFBG), and the linear GD is realized using dispersion compensating fiber (DCF). To reconstruct the input signal from the measured waveform, output complex-field recovery is required followed by digital back-propagation technique. In this demonstration, we used the STARS technique[18] for complex field measurement.

The test input signal was generated using a Mode-Locked Laser (MLL) pulse passed through a highly nonlinear fiber section and filtered using a wavelength division demultiplexer at 1541 nm-1561 nm. The resulted signal was launched into an optical WaveShaper (Finisar 1000 s) to generate the desired test input signal. The test input signal was designed to have a modulation bandwidth of 1000 GHz and duration of 50 ps, see Fig. 4(a). We aim to compress the

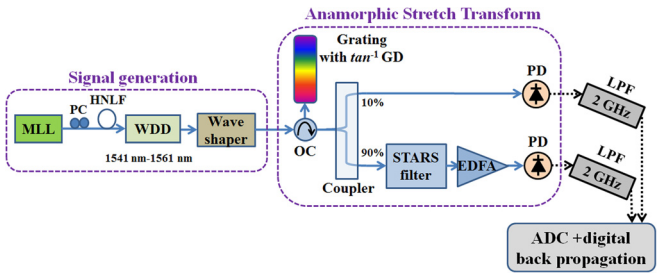

FIG. 2. Experimental setup used for demonstration of analog time-bandwidth compression using AST. AST makes it possible to (i) capture ultrafast signals using a digitizer that otherwise would be too slow and (ii) to alleviate the storage and transmission bottlenecks associated with the resulting big data. It does so by compressing the time-bandwidth product. MLL: mode locked laser, PC: polarization controller, HNLF: highly nonlinear fiber, WDD: wavelength division demultiplexer, OC: optical circulator, GD: group delay, EDFA: Erbium doped fiber amplifier, PD: photo diode, LPF: low pass filter, ADC: analog to digital converter.

input signal envelope (electrical) bandwidth from 1000 GHz to 2 GHz, i.e., a compression factor of 500.

To show the effectiveness of our method, we compare the case of AST using filters with linear GD to the case of nonlinear, specifically inverse tangent ($\tan^{-1}$) GD. The linear case, in the far field, corresponds to coherent dispersive Fourier transform or time stretch transform. For the case of linear GDs, two different modules are used: "Small GD" has total GD equal to that of AST filter and "Large GD" has the same GD slope at the origin. Specifically, Large GD = 25 600 ps^2 and Small GD = 8800 ps^2. For the $\tan^{-1}$ GD, we used the following group delay profile, $\tau(\omega) = A \tan^{-1}(B\ \omega)$, where $A = 5 \times 10^{-9}$ s and $B = 8.7 \times 10^{-13}$ s. AST and both systems with linear GDs in these experiments are operating in the far-field regime. Figure 3 compares the measured filter GDs used in the experiments.[22]

Figure 4(b) compares the measured intensity spectrums. In order to compare the true bandwidth of waveforms, the 2 GHz low pass filter shown in Fig. 2 was not used in these measurements. As clearly seen, the electrical bandwidth in case of Small GD is 5.5 GHz and in cases of Large GD and $\tan^{-1}$ GD is 2 GHz (i.e., the target electrical bandwidth). Figure 4(c) compares the measured output temporal intensity profiles. Here, the 2 GHz electrical low pass filter emulates a system with only 2 GHz analog input bandwidth. In the case of Small GD, the output electrical bandwidth is 5.5 GHz so after the 2 GHz low pass filter, the measured signal has lost its higher frequency features. In cases of Large GD and $\tan^{-1}$ GD, electrical bandwidths are reduced from 1000 GHz to the target 2 GHz, i.e., by 500 times. However, the temporal length, and hence the number of samples needed to represent the signal, is 2.73 times smaller with the $\tan^{-1}$ GD. This clearly demonstrates time-bandwidth compression. The results for AST are single-shot but the large losses in the case of Large GD necessitated signal averaging. Therefore, the results for Large GD are not real-time.

For complex-field measurement, different techniques can be used. Here, we use STARS technique which obtains the

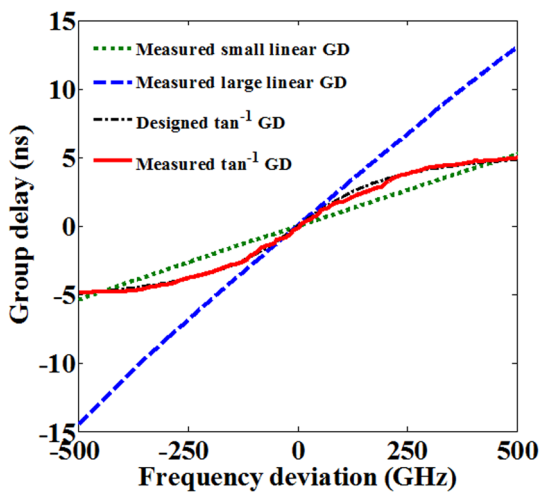

FIG. 3. Comparison of the measured different GDs used in the experiments. The AST uses a sublinear GD realized here using a custom chirped fiber Bragg grating. To show time-bandwidth compression, our results were compared to those that use linear GD: "Small GD" has total GD equal to that of AST filter and "Large GD" has the same GD slope at the origin.

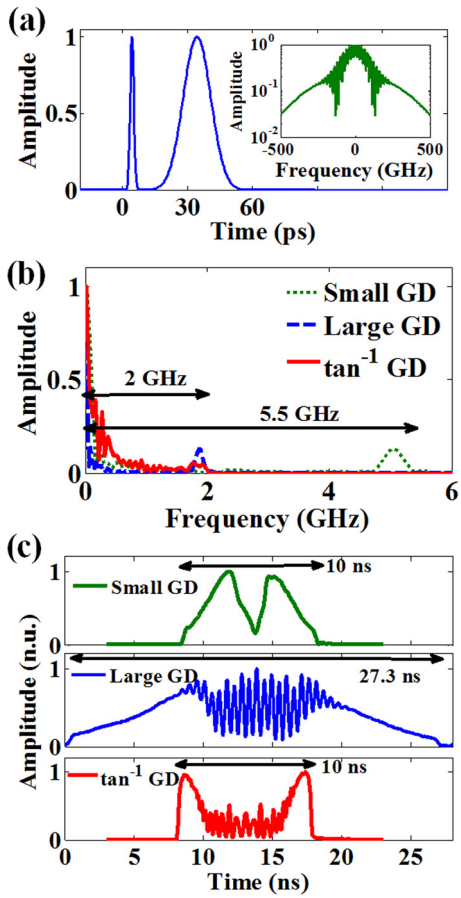

FIG. 4. Experimental demonstration of analog time-bandwidth compression using the AST. (a) Designed input signal, inset shows the spectrum. (b) Comparison of the measured intensity spectrums with linear GD and with $\tan^{-1}$ GD, i.e., AST. Filter GD profiles are shown in Fig. 3. (c) Comparison of the measured temporal outputs after photo detection and the 2 GHz electrical low pass filter. In the case of Small GD, the modulation bandwidth is 5.5 GHz, so after the 2 GHz low pass filter, fast features are lost. In cases of Large GD and $\tan^{-1}$ GD, bandwidths are reduced from 1000 GHz to the target 2 GHz; however, the temporal length is 2.73 times smaller with $\tan^{-1}$ GD. n.u.: normalized unit.

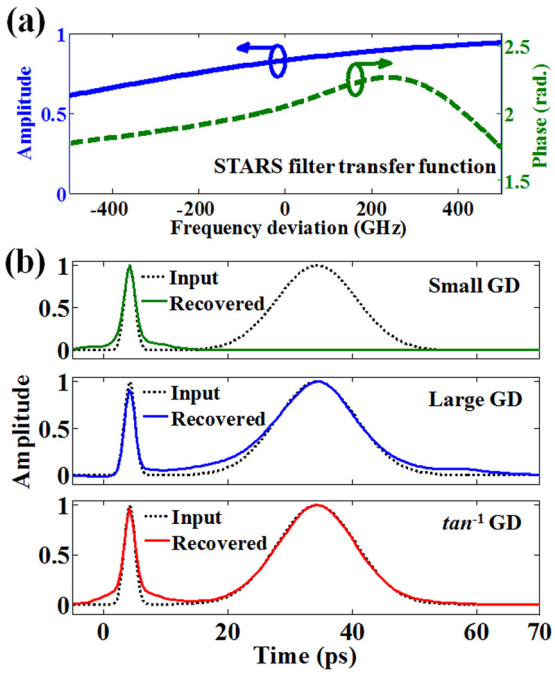

FIG. 5. Experimental demonstration of input signal recovery using AST combined with STARS algorithm. (a) Transfer function of the filter used for STARS complex-field recovery. (b) Comparison of the recovered input signal with the original signal programmed into the WaveShaper. In the case of Small GD, the input signal cannot be recovered because fast features are lost. In cases of Large GD and $\tan^{-1}$ GD, i.e., AST, the input signal is properly recovered; however, the temporal record length is 2.73 times lower with the $\tan^{-1}$ GD.

complex field using two intensity measurements.[18] Using the complex field recovery, the input signal is reconstructed via digital back propagation. Figure 5(a) shows the designed transfer function of the filter used for STARS complex-field recovery. Figure 5(b) compares the recovered input signal with the original signal programmed into the WaveShaper. In the case of Small GD, the input signal cannot be recovered because output fast features are lost (which means long time features in the input signal). In cases of Large GD and $\tan^{-1}$, GD the input signal is properly recovered; however, the temporal record length is 2.73 times lower with the $\tan^{-1}$ GD. We have also calculated the cross-correlation coefficient in each case as a measure of similarity between recovered waveform and target waveform.[23] Specifically, the calculated cross-correlation coefficient for Small GD, Large GD, and $\tan^{-1}$ GD cases were 28%, 89%, and 96%, respectively. The reason that the case with Large GD has worse cross-correlation coefficient than AST case is the ~16 dB higher optical loss in the case of Large GD caused by the dispersive element. This shows the recovered signal using AST has the best correlation to the input signal.

The reduction in time duration using AST results in higher peak power making the detection easier. Also, in the case of Large GD, the loss of the dispersive element is about 18 dB compared to about 2 dB for the inverse tangent filter. In fact, to observe the signal in the case of Large GD, the signal had to be averaged 4000 times. Therefore, while the Large GD reduces the electrical bandwidth, it has much lower signal to noise ratio than in the case of $\tan^{-1}$ GD. Figure 6 summarizes the performances of the AST and TST (i.e., with linear GD) systems to reduce the modulation bandwidth of input signal in these experiments.

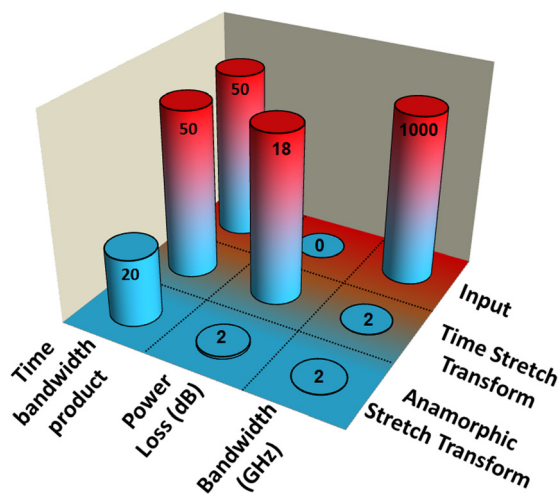

FIG. 6. Comparing the performances of AST and TST, i.e., system with linear group delay. Both can be used to reduce the envelope bandwidth; however, AST results in a shorter record length and better power efficiency. AST compresses the signal time-bandwidth product so the volume of the digital data to represent the signal is reduced.

[1]P. Kelkar, F. Coppinger, A. S. Bhushan, and B. Jalali, Electron. Lett. **35**, 1661 (1999).
[2]M. A. Muriel, J. Azana, and A. Carballar, Opt, Lett. **24**, 1 (1999).
[3]J. Azaña, L. R. Chen, M. A. Muriel, and P. W. E. Smith, Electron. Lett. **35**, 2223 (1999).
[4]D. R. Solli, C. Ropers, P. Koonath, and B. Jalali, Nature **450**, 1054 (2007).
[5]B. Wetzel, A. Stefani, L. Larger, P. A. Lacourt, J. M. Merolla, T. Sylvestre, A. Kudlinski, A. Mussot, G. Genty, F. Dias, and J. M. Dudley, Sci. Rep. **2**, article number: 882 (2012).
[6]F. Qian, Q. Song, E. Tien, S. K. Kalyoncu, and O. Boyraz, Opt. Commun. **282**, 4672 (2009).
[7]C. Zhang, Y. Qiu, R. Zhu, K. K. Y. Wong, and K. K. Tsia, Opt. Express **19**, 15810 (2011).
[8]T. T. W. Wong, A. K. S. Lau, K. K. Y. Ho, M. Y. H. Tang, J. D. F. Robles, X. Wei, A. C. S. Chan, A. H. L. Tang, E. Y. Lam, K. K. Y. Wong, G. C. F. Chan, H. C. Shum, and K. K. Tsia, Sci. Rep. **4**, 3656 (2014).
[9]G. C. Valley, Opt. Express **15**, 1955 (2007).
[10]J. Stigwall and S. Galt, J. Lightwave Technol. **25**, 3017 (2007).
[11]W. Ng, T. D. Rockwood, G. A. Sefler, and G. C. Valley, IEEE Photonics Technol. Lett. **24**, 1185 (2012).
[12]J. Chou, O. Boyraz, D. Solli, and B. Jalali, Appl. Phys. Lett. **91**, 161105 (2007).
[13]R. Solli, S. Gupta, and B. Jalali, Appl. Phys. Lett. **95**, 231108 (2009).
[14]F. Li, Y. Park, and J. Azana, J. Lightwave Technol. **27**, 4623 (2009).
[15]M. H. Asghari, Y. Park, and J. Azana, Opt. Express **18**, 16526 (2010).
[16]C. Wang and J. P. Yao, J. Lightwave Technol. **29**, 789 (2011).
[17]R. P. Scott, N. K. Fontaine, D. J. Geisler, and S. J. B. Yoo, IEEE Photon. J. **4**, 748 (2012).
[18]M. H. Asghari and B. Jalali, IEEE Photon. J. **4**, 1693 (2012).
[19]M. H. Asghari and B. Jalali, Appl. Opt. **52**, 6735 (2013).
[20]B. Jalali and M. H. Asghari, Opt. Photonics News **25**, 24 (2014).
[21]M. H. Asghari and B. Jalali, in IEEE Global Signal and Information Processing Symposium 2013, Austin, Texas, 3–5 December 2013 (NSSIMb.PD.2).
[22]M. H. Asghari and B. Jalali, in Frontiers in Optics 2013, Orlando, Florida, 6–10, October, 2013, Postdeadline Session I (FW6A).
[23]A. Papoulis, *The Fourier Integral and its Applications* (McGraw-Hill, New York, 1962).